Amplification of extreme-ultraviolet radiation in a gas-liner pinch plasma

S. Glenzer and H.-J. Kunze
Institut für Experimentalphysik V, Ruhr-Universität, D-44780 Bochum, Federal Republic of Germany
(Received 31 August 1993)

The emission of the $4f$-$3d$ and of the $4d$-$3p$ spectral lines of the Li-like ions C IV, N V, O VI, and F VII is studied in a gas-liner pinch plasma. For O VI the comparison of radial and axial line intensities reveals clearly amplification of the $4f$-$3d$ transition at 51.97 nm in the axial direction corresponding to a gain-length product of $G = gl = 4.5$. The corresponding transition in F VII at 38.18 nm is enhanced already in the radial direction by factors up to 4.6. The strongest amplification always occurs at times shortly before maximum pinch compression.

PACS number(s): 52.25.Qt, 42.55.Lt, 32.30.Rj

I. INTRODUCTION

The $4f$-$3d$ spectral lines of Li-like ions emitted by dense plasmas are the subject of extensive studies for the generation of short-wavelength lasers. Line-focused laser-produced plasmas were most successful so far. The first observations of a population inversion between the $n = 4, 5$ and $n = 3$ levels of Li-like Al were reported by Kononov *et al.* [1] in a recombining laser-produced plasma. They employed a neodymium-glass laser with power densities of $(1 - 2) \times 10^{13}$ W/cm^2 and a pulse length of 5 ns. Milchberg *et al.* [2] found population inversion between the $4d$ and $3d$ levels for C IV, O VI, F VII, and Ne VIII using a CO_2 laser with a power density of $10^{11} - 10^{12}$ W/cm^2 and 60–80 ns pulse width. For these ions the energy separation of the $4d$ and $4f$ levels is smaller than 500 cm^{-1}, and high electron-collision rates will equalize the population of the $4d$ and $4f$ sublevels. Gain is expected for the $4f$-$3d$ transition, since this transition in the Li-like electronic structure has the advantage of a relative high atomic transition probability in comparison with other $n = 4$ to $n = 3$ transitions, and the lower level has a fast radiative decay $3d$-$2p$. However, no gain was observed experimentally in Refs. [1, 2], because no elongated laser-produced plasma could be generated [1] and no suitable spectrometer in the extreme ultraviolet (xuv) was available [2].

Measurements of gain of the $4f$-$3d$ or of the $5f$-$3d$ transition in Li-like Al are reported in Refs. [3–10]. Population inversion is achieved by fast three-body recombination of He-like ions in laser-produced plasmas. High-n quantum number levels are favored followed by collisional-radiative decay to lower levels. Therefore, ultrashort (0.12–25 ns) high-power ($0.6 \times 10^{11} - 8 \times 10^{13}$ W/cm^2) laser pulses are requested in order to obtain a dense, rapidly cooling plasma. Theoretical simulations [11] of the experiments of Ref. [4] show good agreement with measured gain values, when laser pulses with a time duration shorter than 1 ns are considered. However, measured gain values obtained with long driving laser pulses ($\sim$ 4 ns) are not understood (see also [12]). Furthermore, the predicted gain ratio of the $4f$-$3d$ to the $5f$-$3d$ transitions of about $5 - 10$ could not be observed experimentally.

Based on investigations of Macklin *et al.* [13], where the $4f$-$3d$ spectral line in Li was found to be a laser transition in a recombining metal-vapor arc plasma, Li-like C was investigated in a recombining θ-pinch plasma [14, 15]. The authors found population inversion between the $n = 4, 5$ and $n = 3$ levels. However, the single-pass gain G of the $4f$-$3d$ and $5g$-$4f$ transitions in C IV was too small for lasing without a cavity. This is because of the large ion temperature and modest populations of the excited levels. Furthermore, cavity operation failed because of cavity losses and window absorption. Again three-body recombination was proposed to be the dominant mechanism for establishing the population inversion. However, charge exchange with neutral hydrogen is also advanced as a possible dominant recombination mechanism [15, 16].

In the present paper the $4f$-$3d$ transition of C IV, N V, O VI, and F VII has been investigated in the plasma produced by the gas-liner pinch device. Several requirements for lasing in the xuv spectral region [17] such as high pumping power, high densities of the emitting ions, moderate electron-collision probabilities in comparison to the Einstein A coefficients, and a plasma of appreciable size are easily fulfilled. On the other hand, temperature requirements for lasing, e.g., of H-like ions [18] in the recombination scheme or of collisionally excited Ne-like ions [19] are hard to meet. Because of their smaller ionization potential Li-like and Ni-like ions are thus better candidates for lasing at short wavelength than the lasing transitions in H-like and Ne-like ions, see, e.g., Refs. [20, 21].

It is an essential feature of the present study that we had the capability to investigate ions along the Li-like isoelectronic sequence under similar plasma conditions in order to find suitable spectral lines for lasing in the xuv spectral region. This is of importance because lasing in the recombination scheme requires a collision limit below the upper level of the lasing transition, which is thus rapidly populated, and a strong depopulation of the lower lasing level due to fast radiative decay [17, 22]. The atomic transition probability of the $3d$-$2p$ transition becomes larger along the sequence in comparison to the electron-collision probabilities of the inverse process. Furthermore, the collision limit and the quantum number of the most populated ionic level due to atom-

 ©1994 The American Physical Society

ion charge transfer also increase with the spectroscopic charge number Z [23, 17].

II. EXPERIMENT

Pulsed-power axial discharges have been proposed as active media for short-wavelength lasers by several authors, e.g., [24, 25]. In Ref. [26] a krypton gas puff plasma is investigated for the generation of population inversion in Ne-like krypton by electron-impact excitation. Population inversion by resonant photopumping in the sodium-neon x-ray laser scheme is reported in Ref. [27]. Recently, charge exchange processes in axial discharges between ionic species are proposed to create population inversion because of the selective population of ionic levels [28].

The measurements of the present study are performed with the gas-liner pinch device [29–31]. It resembles a large aspect ratio z-pinch discharge (diameter of the discharge chamber is 18 cm and electrode separation is 5 cm) characterized by two independent special gas inlet systems (Fig. 1). The so-called driver gas (for our measurements we used hydrogen) is injected with a fast electromagnetic valve through an annular nozzle into the vacuum chamber. Initially, the gas builds a hollow gas cylinder near the wall. It is preionized by discharging a 50 nF, 20 kV capacitor through 50 needles mounted annularly below the lower cathode, and it is compressed to a plasma column of 1–2 cm diameter and 5 cm length by discharging the main capacitor bank (11.1 μF, charging voltage: 30–35 kV) through the ionized gas.

A second electromagnetic valve injects the so-called test gas through a nozzle in the center of the upper electrode along the axis of the discharge tube. The gas is dissociated and ionized by the imploding driver gas and by Ohmic heating. We used CH_4, N_2, CO_2, and a 10% mixture of SF_6 in H_2 for the generation of C IV, N V, O VI, and F VII ions, respectively. In contrast to previous investigations (for example, Ref. [32]) a large amount of test gas was injected in order to achieve a high concentration of emitters along the plasma column for a large single-pass gain. With these discharge conditions the test gas ions are no longer distributed homogeneously in the plasma column. However, the investigated line radiation emitted transversely to the plasma column was not affected by self-absorption as will be shown later.

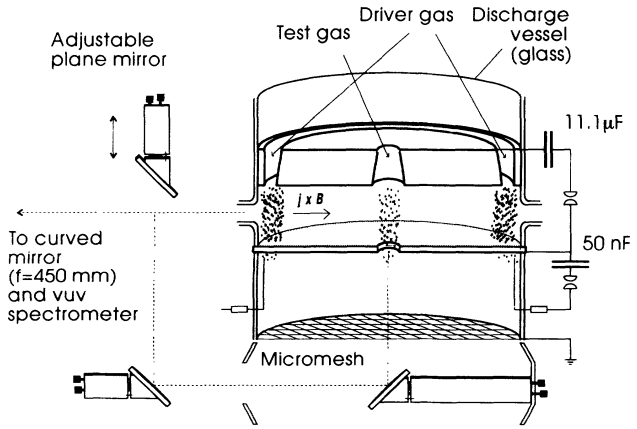

FIG. 1. Schematic of the gas-liner pinch.

The implosion time of the discharge is 1–2 μs and the lifetime of the plasma is shorter than 0.3 μs. The discharge current is monitored with a Rogowski coil and the plasma radiation at 520 nm with a $\frac{1}{4}$-m monochromator equipped with an RCA 1P28 photomultiplier. The plasma parameters in the center of the discharge measured by Thomson scattering [33, 34] were in the range between $1.5 < n_e < 6 \times 10^{18}$ cm^{-3} and $7.5 < kT_e < 45$ eV. These temperatures are high enough for the generation of a considerable amount of ions in the He-like ground state (in the compression phase of the discharge), but still too low to excite a considerable number of these ions to the first excited state. This is because of the large energy separation between the He-like ground state and the first excited level (the ionization potential of He-like C, N, O, and F is larger than the ionization potential of Li-like C, N, O, and F by about a factor of 5). A high initial population density of the He-like ground state level is essential in order to achieve population inversion by recombination processes.

The plasma is accessible through four ports in the midplane of the discharge chamber for side-on observations, and through a hole in the lower cathode of about 1.8 cm diameter opposite to the test gas injection for end-on observations. All measured transitions are in the vacuum ultraviolet (vuv) spectral range and are detected with a 1-m normal-incidence spectrometer (McPherson model 225 with a 1200-line/mm grating blazed at 120 nm). Underneath the discharge is a set of three plane mirrors (MgF_2 on duran glass), set at 45° angle to the incident radiation, to guide the light onto a curved mirror ($f = 450$, MgF_2 on Al) which focuses the emission of the plasma column onto the entrance slit (30 μm width and 2 mm height) of the spectrometer for end-on observations (see Fig. 1). Side-on observations are performed with the curved mirror alone. The distance of the lower electrode to the first plane mirror underneath the lower electrode is about 50 cm and that mirror is protected from plasma bombardment by a grounded micromesh. The spectrometer is equipped with a microchannel plate (MCP) of the Chevron type with CsI coating on the input side and a P20 phosphor at the exit side (Galileo model CEMA 3025). The phosphor screen is imaged onto an optical multichannel analyzer (OMA, EG&G model 1420) giving a reciprocal linear dispersion of 0.021 nm/channel and a full width at half maximum (FWHM) of the Lorentzian apparatus profile of 0.18 nm. Spectra are recorded at various times of the discharge, the gate duration being 20 ns.

For higher time resolution the MCP-OMA system was replaced by a slit in the exit plane of the spectrometer and an XP2972 photomultiplier. The photomultiplier signal was recorded with a Gould oscilloscope (DSO 4094) with 800 Ms/s giving a time resolution of 5 ns. For these measurements the width of the entrance slit was increased to 100 μm, and the width of the exit slit was chosen to be 100 μm or 210 μm so that line radiation integrated over the line profile is detected.

Simultaneously to the observations in the vuv, plasma parameters in the center of the plasma are determined by 90° Thomson scattering. Scattered light of a Korad Q-switch-driven ruby laser pulse (2.5 J, 25 ns) is detected with a 1-m Czerny-Turner spectrometer (Spex model 1704) which is equipped with a second OMA (EG&G model 1456B-990G) system in the exit plane. Details of the experimental procedures are given in Refs. [33, 35]. We modified [34] the theoretical form factor function of Evans [36] in order to allow the determination of electron-proton drifts in the plasma which give rise to asymmetric Thomson scattering profiles. This function is fitted to the experimental spectra by a least-squares procedure [37] giving electron densities, proton, electron, and test gas ion temperatures, the concentration of the test gas ions in the plasma, and drift velocities. In this way it is verified that the concentration of the test gas ions in the center of the plasma is of the order of 10% of the electron density; the mean spectroscopic charge number, which has to be known, is estimated by spectroscopic measurements. When F VII ions were investigated, large asymmetries of the measured Thomson scattering spectra were found, which indicate drift velocities of the order of the compression velocity of the driver gas, $v_c \simeq 5 \times 10^6$ cm/s. In discharges with oxygen as test gas, asymmetries were also present but smaller. On the other hand, the origin of these asymmetries is not clear at all and they are studied in further investigations.

Finally, the whole plasma column is imaged side on through four pinholes (300 μm diameter) onto a four-frame camera system [38]. This system consists of a MCP with a CsI coating and a phosphor screen with four independent sectors and a pulse generator. Each sector is gated separately with a time duration of 5 ns, and the time duration between the triggers of two sectors is 7.5 ns. The phosphor screen is imaged onto a Kodak T-MAX 3200 film. Thus time-resolved pictures of the plasma spectrally integrated over the x-ray and vuv spectral regions are obtained. Taking such pictures with and without the injection of test gas shows that the light emission of free-free, free-bound, and bound-bound transitions of the pure hydrogen plasma is rather small in comparison to the radiation when high-Z ions are present in the plasma.

III. EXPERIMENTAL RESULTS AND DISCUSSION

A. N V and C IV

We measured the relative intensities of the $4f$-$3d$ and $4d$-$3p$ spectral lines (integrated over the line profiles) of N V at 74.83 nm and 71.38 nm side on and in axial direction of the plasma column. By recording the continuum radiation from pure discharges in hydrogen with no test gas injected it was shown that the sensitivity of the vuv detection system was practically constant over those small spectral ranges where respective measurements were done. This procedure was also used to check for unwanted impurities in the plasma. Obtained spectra are shown in Fig. 2. The experimental intensity ratio

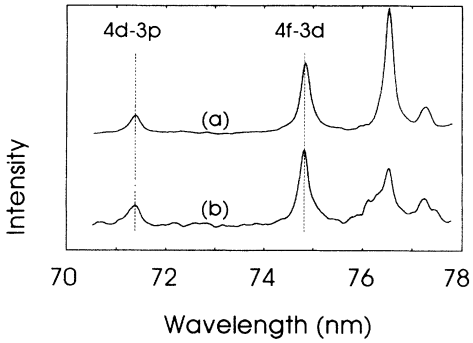

FIG. 2. Example of recorded line spectra of the $4f$-$3d$ and $4d$-$3p$ transitions in N V. Trace (a) is measured side on and trace (b) end on.

$I(4f\text{-}3d)/I(4d\text{-}3p)$ of the side-on emission is independent of the plasma condition and is determined from trace (a) of Fig. 2 to

$$\left(\frac{I(4f\text{-}3d)}{I(4d\text{-}3p)}\right)_{\text{trans}} = 3.1(\pm 7\%). \tag{1}$$

The error is the rms value from about 20 discharges. Line emission of the $2s^2 2p$-$2s 2p^2$ transitions at 76.33 nm and at 76.44 nm and of the $2s 2p^2$-$2p^3$ transitions at 77.2 nm from N III and of the $2s^2$-$2s 2p$ transition at 76.52 nm from N IV ions is also evident.

Because of the small energy gap between the $4d$ and $4f$ levels of 139 cm^{-1} [39] electron collisions between both levels are faster than radiative decay by a factor of about 200 at our densities [40, 41], the population densities of both levels are according to a Boltzmann distribution (see, e.g., Chapter 6 of [23]), and the theoretical intensity ratio of the two lines I and I' is given by (Chapter 13 of [23])

$$\frac{I}{I'} = \frac{\lambda'^3}{\lambda^3}\,\frac{gf}{g'f'}\,\exp\left(\frac{E'-E}{kT_e}\right), \tag{2}$$

where I, λ, g, f, and E are total intensity (integrated over the line profile), wavelength, statistical weight of the lower state of the line, absorption oscillator strength, and excitation energy for the upper level of the line, respectively. This gives an equilibrium intensity ratio of

$$\left(\frac{I(4f\text{-}3d)}{I(4d\text{-}3p)}\right)_{\text{eq}} = 2.64 - 2.69 \tag{3}$$

for electron temperatures above 1 eV. Since it is shown experimentally that this line pair is not affected by self-absorption by measuring the $3s$-$3p$ lines of N V at 460.374 nm and 461.997 nm in the visible spectral range (see also the experimental results of Ref. [32]), and assuming *ad hoc* that there is no amplification of those lines transversely to the plasma column, the slightly differing results of Eqs. (1) and (3) may come from inaccurate Einstein A coefficients of Refs. [41, 42]. Trace (b) of Fig. 2 gives the same intensity ratio of the emission in axial direction:

$$\left(\frac{I(4f\text{-}3d)}{I(4d\text{-}3p)}\right)_{\text{axial}} \leq 3.1. \tag{4}$$

The $\leq$ symbol indicates that some of the axially recorded spectra were self-absorbed due to a cold plasma boundary layer underneath the lower electrode. The effect of self-absorption could also be seen as broadening of the line profiles of the measured transitions [43].

The measurements of the respective lines in C IV give similar results, although the error was somewhat larger due to close-by transitions from C III. Both results show that for Li-like N and C no population inversion is detectable.

B. O VI

Relative intensities of the $4f$-$3d$ and $4d$-$3p$ spectral lines (integrated over the line profiles) of O VI at 51.79 nm and 49.83 nm are also measured transversely and axially to the plasma column with the vuv detection system. We find side on [see trace (a) of Fig. 3] from 30 measurements

$$\left(\frac{I(4f\text{-}3d)}{I(4d\text{-}3p)}\right)_{\text{trans}} = 2.8 - 4.7. \tag{5}$$

The larger measured intensity ratios indicate a small enhancement of the $4f$-$3d$ transition in comparison to the $4d$-$3p$ transition, since the equilibrium considerations predict $[I(4f\text{-}3d)/I(4d\text{-}3p)]_{\text{eq}} = 2.62 - 2.68$ for electron temperatures higher than 1 eV. The axial emission, on the other hand, gives [see trace (b) of Fig. 3]

$$\left(\frac{I(4f\text{-}3d)}{I(4d\text{-}3p)}\right)_{\text{axial}} \approx 25. \tag{6}$$

This large enhancement of the axial emission of the $4f$-$3d$ spectral line in comparison to the $4d$-$3p$ spectral line in contrast to the side-on observation is obvious from Fig. 3. This effect is not due to self-absorption of the measured lines, because the optical depth of the $4f$-$3d$ spectral line is larger than that of the $4d$-$3p$ line (Chapter 7 of [23]) at our plasma conditions, and any optical depth effect will reduce the intensity ratio. The enhancement is observed at times around maximum pinch compression and just before. During a time interval of 130 ns 16 measurements show clearly an enhancement and 34 do not. Individual spectra show even a higher enhancement than quoted in Eq. (6); nevertheless, we derived the enhancement by averaging over the 16 spectra for better reliability. The relative high intensities of the O III $2s^22p^2$-$2s2p^3$ spectral lines at 50.8 nm and 52.6 nm and of the O IV $2s^23p$-$2p^23s$ spectral lines at 53.6 nm of the axial emission in Fig. 3 are from a cold plasma layer underneath the lower electrode. We derive an enhancement E due to laser action for the $4f$-$3d$ line of O VI with

$$E = \frac{I(4f\text{-}3d)_{\text{axial}}}{I(4f\text{-}3d)_{\text{trans}}} \left(\frac{I(4d\text{-}3p)_{\text{axial}}}{I(4d\text{-}3p)_{\text{trans}}}\right)^{-1}. \tag{7}$$

In the case of a Doppler profile the enhancement E is related to the single-pass gain $G = gl$ [44, 45],

$$E = \frac{I}{I_0} = \left(\frac{\exp(gl) - 1}{gl}\right)^{3/2} \left(\frac{1}{\exp(gl)}\right)^{1/2}, \tag{8}$$

where g is the small-signal coefficient and l is the length of the lasant plasma. This gives $G = gl = 4.5$ for our experimental results of O VI. The true gain, however, could be even larger, because in the case of equilibrium population between the $4f$ and $4d$ levels and the $3d$ and $3p$ levels, respectively, the $4d$-$3p$ spectral line should also exhibit laser action. Assuming an inversion factor of $F = 1/3$ and $kT_e = 10$ eV, we find for O VI

$$\frac{G(4f\text{-}3d)}{G(4d\text{-}3p)} \approx 3.6. \tag{9}$$

A similar statement has been given in Ref. [6]. On the other hand, it was experimentally observed that the gain of the $4f$-$3d$ and of the $4d$-$3p$ transition of Al XI was about equal (e.g., [5]).

The spectra in Figs. 2 and 3 are time integrated over 20 ns, and it is conceivable that the instantaneous gain could be higher during that time interval. For this reason we performed time-resolved measurements of the radial and axial emission of the O VI $4f$-$3d$ and $4d$-$3p$ line pair with an XP2973 photomultiplier. Line intensity ratios of the transverse emission of the $4f$-$3d$ to the $4d$-$3p$ spectral lines are in the range of $2 - 4$. The reproducibility of the absolute line intensities and of the continuum emission is rather poor side on and even worse for the axial emission. For this reason no enhancement is being derived as was done from the spectra, since intensities of the two lines from successive discharges have to be compared. However, axial signals show an emission burst of the $4f$-$3d$ spectral line. Detected signals of the transverse (a) and the axial (b) emission of that line together with the plasma continuum radiation at 520 nm (c) are plotted in Fig. 4. The axial emission peaks about 75 ns after the maximum emission of the transverse signal. From 32 measurements nine signals indeed show bursts on the axial signal in the time region 140 ns$\leq t \leq$ 200 ns, that is, at the same time when the OMA measurements show the large enhancement of the axial emission. On the signals of the $4d$-$3p$ emission line no burst was detectable.

Extrapolating the intensity I_0 of the axial emission from times, where no bursts occur, and integrating the burst, which has a time duration of the minimum possible detectable signal, gives an enhancement for the pho-

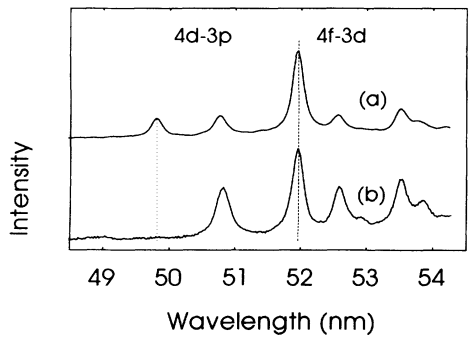

FIG. 3. Example of recorded line spectra of the $4f$-$3d$ and $4d$-$3p$ transitions in O VI. Trace (a) is measured side on and trace (b) end on.

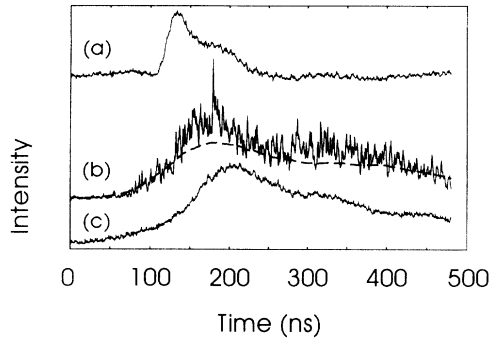

FIG. 4. Line intensity of the $4f$-$3d$ transition in O VI (a) side on without continuum and (b) end on with continuum (indicated by the dashed curve which is obtained by adaptive smoothing of the continuum signal [46]) as a function of time. Trace (c) shows the continuum radiation at 520 nm.

tomultiplier measurements of

$$E = \frac{I}{I_0} = 6.1. \tag{10}$$

This corresponds to $G = gl = 3.9$. This result is somewhat smaller than the result of the OMA-MCP measurements. One reason could be the poor reproducibility of the absolute end-on signals, which makes it difficult to substract the continuum emission from the line emission.

The population inversion should depend on the plasma parameters, and in order to identify this we performed spectroscopic line intensity measurements of the transverse emission simultaneously with Thomson scattering. Figure 5 shows the result: the side-on intensity ratio is plotted as a function of the electron density. The electron temperature was in the range $10 - 17$ eV. The collision limit n^* calculated according to Ref. [23] for a temperature of $kT = 15$ eV is quoted for each density. The density effect is evident. The largest enhancement is seen with the lowest density corresponding to a collision limit of $n^* \simeq 3.7$. Increasing electron density increases the collisional coupling between the levels and by fitting a linear curve to the experimental values we find that for $n_e \approx 5.2 \times 10^{18}$ cm^{-3} corresponding to a collision limit of $n^* = 3.4$ for $kT_e = 15$ eV the equilibrium intensity ratio of $[I(4f\text{-}3d)/I(4d\text{-}3p)]_{\text{eq}} = 2.68$ is matched.

The values of the collision limit indicate that the $n = 4$ levels should be in equilibrium, and hence the enhanced intensity ratios can only be explained with some amplification of the $4f$-$3d$ emission transverse to the plasma axis. Our plasma parameters themselves are indeed most favorable for lasing according to the recombination scheme [17], the major problem being the rapid cooling of the hot plasma, which has to precede lasing in order that three-body recombination is most effective in producing the population inversion. Although temperatures measured in the center of the plasma column by Thomson scattering do not show this cooling, it is generally accepted [47] that in z-pinch implosions a high-density and high-temperature narrow plasma channel of very short duration can be produced, when the imploding plasma converges first on the axis: the channel disappears very quickly and is difficult to detect since even Thomson scattering integrates over the duration of the laser pulse and over some plasma volume. The existence might show up, however, on large variations of the plasma parameters from discharge to discharge, and it is indeed observed that the rms deviations increase by a factor of 2 at respective times.

We finally were interested in the spatial distribution of the oxygen ions. For this purpose we observed the plasma column through four pinholes. The pinhole pictures were detected with the four-frame microchannel plate; the image separation was 7.5 ns. Figure 6 shows four such images indicating the oxygen distribution from 50 ns to 20 ns before maximum pinch compression. The length of the plasma column seen is 4 cm. It is obvious that probably Rayleigh-Taylor instabilities develop during the implosion [48]. They are not seen in discharges without oxygen or low oxygen concentration.

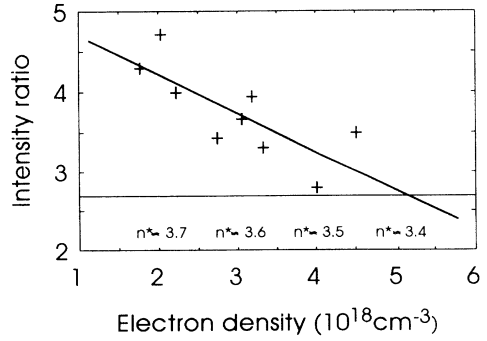

FIG. 5. Line intensity ratio of the $4f$-$3d$ to the $4d$-$3p$ transitions in O VI as a function of the electron density. Also given is the value of the intensity ratio (straight line) after the equilibrium relation [Eq. (2)], a linear least-squares fit to the experimental ratios, and the collision limit n^* after Ref. [23].

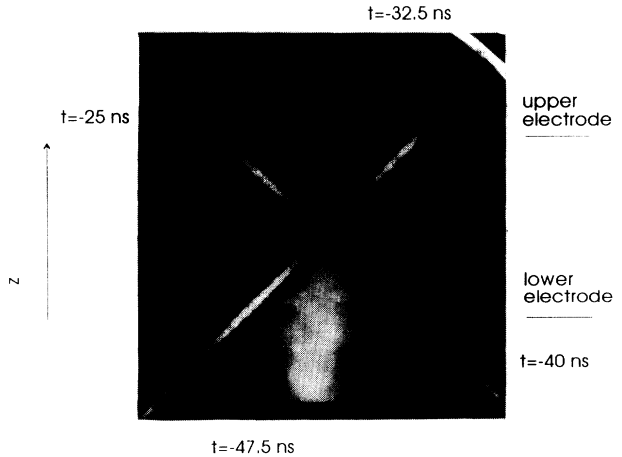

FIG. 6. Example of pinhole pictures recorded from 50 to 20 ns before maximum pinch compression. The existence of Rayleigh-Taylor instabilities is evident in the emission from oxygen ions. The higher brightness of the first picture is instrumental.

C. F VII

The $4f$-$3d$ and the $4d$-$3p$ spectral lines of F VII at 38.2 nm and 36.8 nm were only investigated transversely to the plasma column, because the reflectivity of the mirrors was too low in the wavelength range below 40 nm to detect the axial emission. The discharge voltage was increased to 35 kV for these experiments. We find a similar effect for the line intensity ratio of the $4f$-$3d$ to the $4d$-$3p$ spectral lines as in the case of O VI. However, the enhancement of the $4f$-$3d$ line is much larger. Figure 7 shows two spectra in the range of 35.5–40.5 nm obtained for the same time ($t = 40$ ns before maximum pinch compression). Some evidence of the S VI $4s$-$3p$ doublet is found at 38.89 nm and at 39.09 nm. Again enhancement occurs briefly before and at the time of maximum pinch compression. We find for different discharges

$$\left(\frac{I(4f\text{-}3d)}{I(4d\text{-}3p)}\right)_{\text{trans}} = 2.8 - 13, \tag{11}$$

where the lowest value corresponds again to equilibrium population of the $4f$ and $4d$ levels. The enhancement of the $4f$-$3d$ line varies strongly from discharge to discharge. The dependence of the intensity ratio on the electron density and on the collision limit is not as obvious as in the case of the results of the O VI emission since no values with a respective collision limit smaller than 3.7 are measured. This is demonstrated in Fig. 8, where the collision limit is calculated for an electron temperature of 30 eV. The actual temperature range of these values is 15–45 eV.

Pinhole pictures of the plasma again revealed the existence of Rayleigh-Taylor instabilities along the axis of the plasma column similar to the case of O VI. In order to investigate the plasma regions where such instabilities occur we performed additionally spectroscopic measurements of the intensity ratio of the $4f$-$3d$ to the $4d$-$3p$ transition in F VII with a charge-coupled-device (CCD) camera (SI model ICCD 576 G/RB) instead of the OMA detector head behind the phosphor screen in the vuv spectrometer. Along the axis of the discharge 36.8 mm were resolved with a resolution of 0.09 mm by that device. In Fig. 9 part of the spectrum is shown. The enhancement of the $4f$-$3d$ emission of F VII is located in

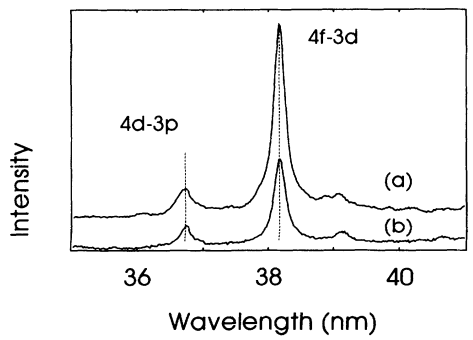

FIG. 7. Two examples of recorded line spectra of the $4f$-$3d$ and $4d$-$3p$ transitions in F VII. Both traces were measured side on for the same time in the discharge.

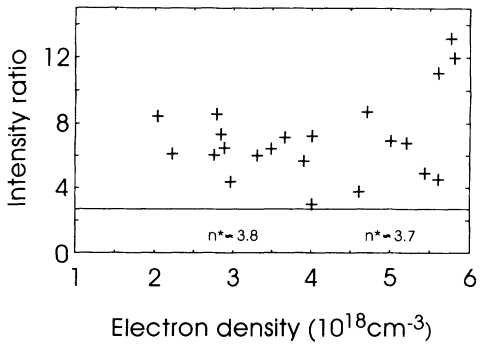

FIG. 8. Line intensity ratio of the $4f$-$3d$ to the $4d$-$3p$ transition in F VII as a function of the electron density. Also given are the values of the intensity ratio according to the equilibrium relation [Eq. (2)] and the collision limit n^* after Ref. [23].

regions of, for example, 0.8 mm height along the axis. This fact is an indication of amplified spontaneous emission [49] transverse to the plasma axis. Furthermore, the observed Rayleigh-Taylor instabilities give rise to different extensions of the plasma in radial direction and hence also explain the large axial variations of the enhancement of the side-on emission as well as the variations from discharge to discharge.

Inhomogeneities in laser-produced plasmas have been investigated by several authors [50–57]. It is stated that the gain of lasing transitions is reduced for the Ne-like collisional excitation scheme, because temperature requirements for lasing are not fulfilled along the full elongated plasma. Refraction effects and turbulent broadening also reduce the gain. For a recombining plasma it is calculated that inhomogeneities along the amplified beam give rise to self-absorption of the lasing transition and also to a reduction of gain. In our experiment, however, electron and ion densities are smaller than in laser-produced plasmas and, following Ref. [17], refraction of the lasing beam out of the gain regions is negligible for densities $n_e \leq 10^{19}$ cm^{-3} and wavelength $\lambda \sim 40$ nm and

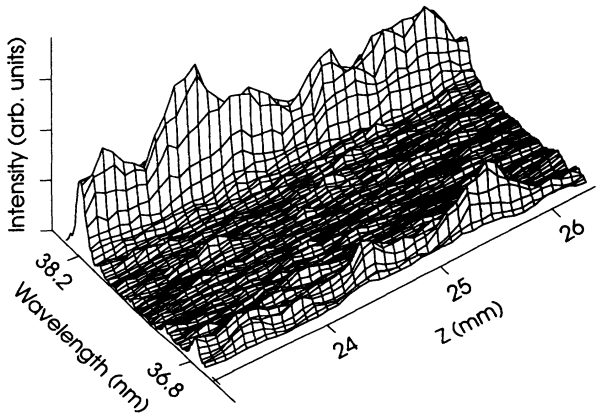

FIG. 9. Example of line spectra recorded with the CCD camera. The intensity ratio of the $4f$-$3d$ to the $4d$-$3p$ transition is enhanced over the equilibrium ratio in regions of about 0.8 mm along the axis.

self-absorption of the lasing transition is not of importance for our conditions.

IV. SUMMARY AND OUTLOOK

We find large gain-length products for the $4f$-$3d$ transition of O VI and F VII emitted from plasmas in the gas-liner pinch discharge. The experimental results show that this discharge type is indeed a promising source for the generation of lasers in the extreme ultraviolet and vacuum ultraviolet spectral range. Measured gain-length products for this transition are comparable with those obtained in laser-produced plasmas.

Three-body recombination most probably is responsible for the observed population inversion, although model calculations carried out for O VI similar to Ref. [11] indicate that cooling times shorter than 1 ns are needed for this pumping scheme to be effective. This is possible immediately after the first compression. In addition an influence of instabilities cannot be ruled out. This and other mechanisms such as charge exchange will be studied in the future.

ACKNOWLEDGMENTS

This research was supported by the Sonderforschungsbereich 191 of the DFG. The authors appreciate helpful comments by H. R. Griem and K. N. Koshelev. We would also like to thank Th. Wrubel, S. Büscher, O. Herzog, and E. Schmieder for their help during various stages of the experiment. We are indebted to R. Schäfer from SI who made the CCD camera available.

[1] E. Ya. Kononov, K. N. Koshelev, Yu. A. Levykin, Yu. V. Sidel'nikov, and S. S. Churilov, Sov. J. Quant. Electron. **6**, 308 (1976).
[2] H. Milchberg, J. L. Schwob, C. H. Skinner, S. Suckewer, and D. Voorhees, in *Laser Techniques in the Extreme Ultraviolet*, edited by S. E. Harris and T. B. Lucatorto (American Institute of Physics, New York, 1984).
[3] G. Jamelot, P. Jaeglé, A. Carillon, A. Bideau, C. Moller, H. Guennon, and A. Sureau (unpublished).
[4] P. Jaeglé, G. Jamelot, A. Carillon, A. Klisnick, A. Sureau, and H. Guennon, J. Opt. Soc. Am. B **4**, 563 (1987); G. Jamelot, A. Klisnick, A. Carillon, H. Guennou, A. Sureau, and P. Jaeglé, J. Phys. B **18**, 4647 (1985); P. Jaeglé, A. Carillon, A. Klisnick, G. Jamelot, H. Guennou, and A. Sureau, Europhys. Lett. **1**, 555 (1986).
[5] J. C. Moreno, H. R. Griem, S. Goldsmith, and J. Knauer, Phys. Rev. A **39**, 6033 (1989).
[6] A. Carillon, M. J. Edwards, M. Grande, M. J. de C. Henshaw, P. Jaeglé, G. Jamelot, M. H. Key, G. P. Kiehn, A. Klisnick, C. L. S. Lewis, D. O'Neill, G. J. Pert, S. A. Ramsden, C. M. E. Regan, S. J. Rose, R. Smith, and O. Willi, J. Phys. B **23**, 147 (1990).
[7] G. Jamelot, A. Carillon, A. Klisnick, and P. Jaeglé, Appl. Phys. B **50**, 239 (1990).
[8] D. Kim, C. H. Skinner, A. Wouters, E. Valeo, D. Voorhees, and S. Suckewer, J. Opt. Soc. Am. B **6**, 115 (1989).
[9] P. X. Lu, Z. Q. Zhang, Z. Z. Xu, P. Z. Fan, S. S. Chen, and B. F. Shen, Appl. Phys. Lett. **60**, 1649 (1992).
[10] J. C. Moreno, H. R. Griem, R. W. Lee, and J. F. Seely, Phys. Rev. A **47**, 374 (1993).
[11] A. Klisnick, A. Sureau, H. Guennou, C. Möller, and J. Virmont, Appl. Phys. B **50**, 153 (1990).
[12] R. Epstein, Phys. Fluids B **1**, 214 (1989).
[13] J. J. Macklin, O. R. Wood II, and W. T. Silfvast, IEEE J. Quantum Electron. **QE-18**, 1832 (1982).
[14] R. U. Datla, J. R. Roberts, W. T. Silfvast, and O. R. Wood II, Opt. Lett. **12**, 675 (1987).
[15] R. U. Datla, S. Eshhar, J. R. Roberts, O. R. Wood II, and W. T. Silfvast, Phys. Rev. A **47**, 1547 (1993).
[16] R. U. Datla and H.-J. Kunze, Phys. Rev. A **37**, 4614 (1988).
[17] R. C. Elton, *X-Ray Lasers* (Academic, New York, 1990).
[18] S. Suckewer, C. H. Skinner, H. Milchberg, C. Keane, and D. Voorhees, Phys. Rev. Lett. **55**, 1753 (1985).
[19] D. L. Matthews, P. L. Hagelstein, M. D. Rosen, M. J. Eckart, N. M. Ceglio, A. U. Hazi, H. Medecki, B. J. MacCowan, J. E. Trebes, B. L. Whitten, E. M. Campbell, C. W. Hatcher, A. M. Hawryluk, R. L. Kauffman, L. D. Pleasance, G. Rambach, J. H. Scofield, G. Stone, and T. A. Weaver, Phys. Rev. Lett. **54**, 110 (1985).
[20] S. Suckewer and C. H. Skinner, Science **247**, 1553 (1990).
[21] B. J. MacGowan, L. B. Da Silva, D. J. Fields, C. J. Keane, J. A. Koch, R. A. London, D. L. Matthews, S. Maxon, S. Mrowka, A. L. Osterheld, J. H. Scofield, G. Shimkaveg, J. E. Trebes, and R. S. Walling, Phys. Fluids B **4**, 2326 (1992).
[22] L. I. Gudzenko and L. A. Shelepin, Sov. Phys. JETP **18**, 998 (1964).
[23] H. R. Griem, *Plasma Spectroscopy* (McGraw-Hill, New York, 1964).
[24] R. W. Lee and A. Zigler, Appl. Phys. Lett. **53**, 2028 (1988).
[25] M. C. Marconi and J. Rocca, Appl. Phys. Lett. **54**, 2180 (1989).
[26] J. Davis, Nav. Res. Rev. **3**, 36 (1989).
[27] J. L. Porter, R. B. Spielman, M. K. Matzen, E. J. McGuire, L. E. Ruggles, M. F. Vargas, J. P. Apruzese, R. W. Clark, and J. Davis, Phys. Rev. Lett. **68**, 796 (1992).
[28] N. K. Koshelev and H.-J. Kunze (unpublished).
[29] K. H. Finken and U. Ackermann, Phys. Lett. **85A**, 278 (1981).
[30] K. H. Finken and U. Ackermann, J. Phys. D **15**, 615 (1982).
[31] H.-J. Kunze, in *Spectral Line Shapes*, edited by R. J. Exton (Deepak, Hampton, VA, 1987), Vol. 4.
[32] S. Glenzer, N. I. Uzelac, and H.-J. Kunze, Phys. Rev. A **45**, 8795 (1992).
[33] A. Gawron, S. Maurmann, F. Böttcher, A.Meckler, and H.-J. Kunze, Phys. Rev. A **38**, 4737 (1988).
[34] S. Glenzer, Th. Wrubel, S. Büscher, and H.-J. Kunze, in *Proceedings of the XXIst International Conference on Phenomena in Ionized Gases, Sept. 19–23, 1993, Bochum*, edited by G. Ecker, U. Arendt, and J. Böseler

(Arbeitsgemeinschaft Plasmaphysik, Bochum 1993), Vol. II, pp. 367 and 368.
[35] A. W. DeSilva, T. J. Baig, I. Olivares, and H.-J. Kunze, Phys. Fluids B **4**, 458 (1992).
[36] D. E. Evans, Plasma Phys. **12**, 573 (1970).
[37] J. E. Dennis, Jr. and D. J. Woods, in *New Computing Environments: Microcomputers in Large-Scale Computing*, edited by A. Wouk (SIAM, Philadelphia, 1987).
[38] Y. V. Sopkin, L. A. Dorokhin, K. N. Koshelev, and Y. V. Sidelnikov, Phys. Lett. A **152**, 215 (1991).
[39] R. L. Kelly, *Atomic and Ionic Spectrum Lines below 2000 Ångströms: Hydrogen through Krypton*, [J. Phys. Chem. Ref. Data **16**, Suppl. 1, 79 (1987)], Part I (H–Cr).
[40] S. M. Younger and W. L. Wiese, J. Quant. Spectrosc. Radiat. Transfer **22**, 161 (1979).
[41] J. D. Hey, S. Afr. J. Phys. **10**, 118 (1987).
[42] W. L. Wiese, M. W. Smith, and B. M. Glennon, *Atomic Transition Probabilities*, Natl. Bur. Stand. (U.S.) No. NSRDS-NBS 4 (U.S. GPO, Washington, DC, 1966), Vol. I.
[43] H. R. Griem, *Spectral Line Broadening by Plasmas* (Academic, New York, 1974).
[44] G. J. Linford, E. E. Peressini, W. R. Sooy, and M. L. Spaeth, Appl. Opt. **13**, 379 (1974).
[45] R. A. London, Phys. Fluids **31**, 184 (1988).
[46] S. Kawata and S. Minami, Appl. Spectrosc. **38**, 49 (1984).
[47] A. Böhnlein, Z. Naturforsch. Teil A **21**, 1660 (1966).
[48] W. W. Hsing and J. L. Porter, Appl. Phys. Lett. **50**, 1572 (1987).
[49] S. Suckewer, C. H. Skinner, D. Kim, E. Valeo, D. Voorhees, and A. Wouters, Phys. Rev. Lett. **57**, 1004 (1986).
[50] H. R. Griem, Phys. Rev. A **33**, 3580 (1986).
[51] T. N. Lee, W. A. Molander, J. L. Ford, and R. C. Elton, Rev. Sci. Instrum. **57**, 3580 (1986).
[52] Z. Z. Xu, P. M. Y. Lee, L. H. Lin, W. Q. Zhang, Z. M. Jiang, S. X. Meng, J. J. Yu, and A. D. Qian, Opt. Commun. **61**, 199 (1987).
[53] M. D. J. Burgess, R. Dragila, B. Luther-Davies, K. A. Nugent, A. J. Perry, G. J. Tallents, M. C. Richardson, and R. S. Craxton, Phys. Rev. A **32**, 2899 (1985).
[54] J. C. Kieffer, M. Chaker, H. Pépin, H. A. Baldis, G. D. Enright, B. Lafontaine, and D. M. Villeneuve, Phys. Fluids B **3**, 463 (1991).
[55] G. D. Enright, D. M. Villeneuve, J. Dunn, H. A. Baldis, J. C. Kieffer, H. Pépin, M. Chaker, and P. R. Herman, J. Opt. Soc. Am. B **8**, 2047 (1991).
[56] P. Jaeglé, G. Abdelatif, A. Carillon, P. Dhez, B. Gauthe, G. Jamelot, A. Klisnick, and J. P. Raucourt, in *Short Wavelength Lasers and their Applications*, edited by V. V. Korobkin and M. Yu. Romanovsky (Nova Science Publishers, New York, 1992).
[57] B. La Fontaine, J. Dunn, H. A. Baldis, G. D. Enright, D. M. Villeneuve, J. C. Kieffer, M. Nantel, and H. Pépin, Phys. Rev. E **47**, 583 (1993).

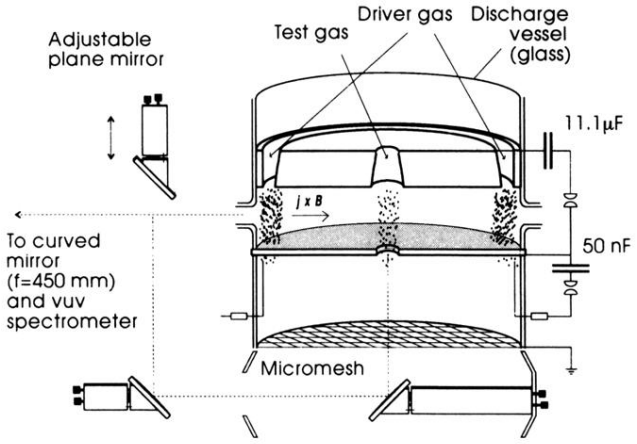

FIG. 1. Schematic of the gas-liner pinch.

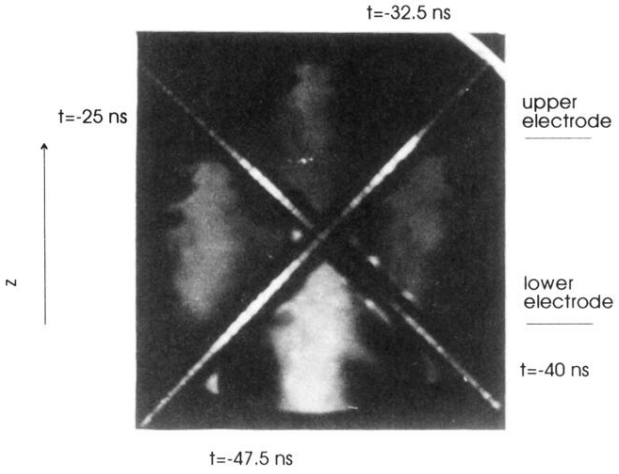

FIG. 6. Example of pinhole pictures recorded from 50 to 20 ns before maximum pinch compression. The existence of Rayleigh-Taylor instabilities is evident in the emission from oxygen ions. The higher brightness of the first picture is instrumental.